

## Accepted Manuscript

*Drosophila* multicopper oxidase 3 is a potential ferroxidase involved in Iron homeostasis

Xudong Wang, Sai Yin, Zhihao Yang, Bing Zhou



PII: S0304-4165(18)30110-7  
DOI: [doi:10.1016/j.bbagen.2018.04.017](https://doi.org/10.1016/j.bbagen.2018.04.017)  
Reference: BBAGEN 29099

To appear in:

Received date: 24 February 2018  
Revised date: 29 March 2018  
Accepted date: 17 April 2018

Please cite this article as: Xudong Wang, Sai Yin, Zhihao Yang, Bing Zhou , *Drosophila* multicopper oxidase 3 is a potential ferroxidase involved in Iron homeostasis. The address for the corresponding author was captured as affiliation for all authors. Please check if appropriate. *Bbagen*(2018), doi:[10.1016/j.bbagen.2018.04.017](https://doi.org/10.1016/j.bbagen.2018.04.017)

This is a PDF file of an unedited manuscript that has been accepted for publication. As a service to our customers we are providing this early version of the manuscript. The manuscript will undergo copyediting, typesetting, and review of the resulting proof before it is published in its final form. Please note that during the production process errors may be discovered which could affect the content, and all legal disclaimers that apply to the journal pertain.

# ***Drosophila* Multicopper Oxidase 3 is a Potential Ferroxidase Involved in Iron Homeostasis**

Xudong Wang, Sai Yin, Zhihao Yang<sup>2</sup>, Bing Zhou<sup>1,3\*</sup>

1. State Key Laboratory Membrane Biology, School of Life Sciences, Tsinghua University, Beijing, 100084, China

2. School of Medicine, Tsinghua University, Beijing, 100084, China

3. Beijing Institute for Brain Disorders, Beijing, China

\*Correspondence: Bing Zhou, Tel: +86-10-62795322, Fax: +86-10-62772253, E-mail: zhoubing@mail.tsinghua.edu.cn

## **Abstract**

Multicopper oxidases (MCOs) are a specific group of enzymes that contain multiple copper centers through which different substrates are oxidized. Main members of MCO family include ferroxidases, ascorbate oxidases, and laccases. MCO type of ferroxidases are key to iron transport across the plasma membrane. In *Drosophila*, there are four potential multiple oxidases, MCO1-4. No convincing evidence has been presented so far to indicate any of these, or even any insect multicopper oxidase, to be a ferroxidase. Here we show *Drosophila* MCO3 (dMCO3) is highly likely a bona fide ferroxidase. *In vitro* activity assay with insect-cell-expressed dMCO3 demonstrated it has potent ferroxidase activity. Meanwhile, the ascorbate oxidase and laccase activities of dMCO3 are much less significant. dMCO3 expression *in vivo*, albeit at low levels, appears mostly extracellular, reminiscent of mammalian ceruloplasmin in the serum. A null *dMCO3* mutant, generated by CRISPR/Cas9 technology, showed disrupted iron homeostasis, evidenced by increased iron level and reduced metal importer *Mvl* expression. Notably, *dMCO3*-null flies phenotypically are largely normal at normal or iron stressed-conditions. We speculate the likely existence of a similar iron efflux apparatus as the mammalian ferroportin/ferroxidase in *Drosophila*. However, its importance to fly iron homeostasis is greatly minimized, which is instead dominated by another iron efflux avenue mediated by the ZIP13-ferritin axis along the ER/Golgi secretion pathway.

**Key Words:** *Drosophila melanogaster*; Multicopper oxidase 3; Ferroxidase; Iron homeostasis

## Introduction

Iron is an essential micronutrient to almost all organisms. It is involved in various biological processes such as oxidative respiration, DNA synthesis, and dopamine production (Andersson et al., 1992; Clark, 1994; Warburg, 1925). At the cellular level, iron exists in the form of ferric iron and ferrous iron. Ferrous iron is a potent catalyst for the Fenton reaction, and could generate hazardous hydroxyl radicals by redox reactions and result in serious damages to various cell components such as lipid, DNA and proteins (Nichol et al., 2002; Sheftel et al., 2012). This property necessitates extra iron to be stored as the ferric form. The ferric iron is highly insoluble *in vivo* and commonly stored in the 24-subunit hollow sphere super complex called ferritin, which acts as an iron storage site as well as a likely iron delivery vehicle when secreted in *Drosophila* (Charlesworth et al., 1997; Li, 2010; Locke and Leung, 1984; Missirlis et al., 2007; Tang and Zhou, 2013a).

Redox cycling of the two forms of iron *in vivo* is catalyzed by ferrireductase and ferroxidase (Kosman, 2010). In ferritin complex, the heavy chain is associated with ferroxidase activity and is responsible for the conversion of ferrous iron to ferric iron to be stored (Bou-Abdallah et al., 2008). Besides this source of ferroxidase, there are two other notable ferroxidases namely ceruloplasmin and hephaestin in mammalian organisms, both belonging to the family of enzymes called multicopper ferroxidase. Ceruloplasmin and hephaestin are two highly similar proteins and function to oxidize ferrous iron to ferric iron, facilitating a membrane transporter called ferroportin to move iron across the plasma membrane for iron efflux (Harris et al., 1999; Vulpe et al., 1999). Ceruloplasmin is primarily a soluble plasma ferroxidase of hepatic origin and plays a role in iron homeostasis in the liver and several other tissues, whereas hephaestin is a membrane protein that is highly expressed in the small intestine, and required for efficient dietary iron absorption. Hephaestin therefore is responsible for the uptake of iron from the diet, whereas ceruloplasmin helps in the redistribution of iron from the liver and other internal organs. These findings linked copper to iron, and led to the realization that copper homeostasis is intimately associated with iron metabolism (Fox, 2003).

A similar multicopper ferroxidase, Fet3p, exists in yeast. However, different with ceruloplasmin and hephaestin in animals for iron transport out of the cell, Fet3p is involved in iron uptake from the outside in yeast cells. In this aspect, the iron import apparatus in yeast, which

requires the coordinated action of multicopper oxidase Fet3 and a membrane permease Ftr1, is somewhat similar to the iron efflux system in mammals (Askwith et al., 1994; Stearman et al., 1996).

It is not known whether a similar multicopper ferroxidase/ferroportin iron efflux system exists in insects. *Drosophila melanogaster*, for example, lacks a sequence-similar protein to mammalian ferroportin in the genome. This is partially sensible since iron homeostasis in *Drosophila* differs from that of mammals; Although in mammals iron efflux is generally carried out by the multicopper ferroxidase/ferroportin system, in the fly iron is exported primarily, if not entirely, by ferritin secretion (Calap-Quintana et al., 2017; Mandilaras et al., 2013; Tang and Zhou, 2013b). In contrast to its predominantly cytosol-resident mammalian counterpart, *Drosophila* ferritin is secreted, thereby leading to iron excretion. In this scenario, fly ZIP13 (dZIP13) effluxes iron to the ER/Golgi secretion pathway, and the iron is then loaded to ferritin and subsequently secreted to the circulation for systemic use. Loss of dZIP13 or ferritin in *Drosophila* gut results in systemic iron deficiency (Tang and Zhou, 2013a; Xiao et al., 2014).

Nevertheless, there are four MCO genes (*MCO1-4*) in the *Drosophila melanogaster* genome that are homologous to ceruloplasmin/hephaestin (Dittmer and Kanost, 2010). The path to search for a MCO type ferroxidase in insects was not smooth. Of the four MCO proteins, MCO1 was initially been reported to be a ferroxidase, but later turned out to possess very low ferroxidase activity. Instead, MCO1, including its counterpart from *Anopheles gambiae*, was shown to be a potent ascorbate oxidase (Lang et al., 2012; Peng et al., 2015). MCO2 is predicted to be a laccase and the function of MCO4 remains unclear (Dittmer and Kanost, 2010). Notably based on sequence comparison, *Dan Kosman* a few years before supposed that the fly MCO3 (dMCO3) might be a ferroxidase and consistently *Fanis Missirlis* with coworkers showed that one *dMCO3* mutant allele, *MCO3<sup>C359</sup>*, accumulated more iron in the iron cell region of the midgut (Bettendi et al., 2011; Folwell et al., 2006). Overall, no MCO candidates have ever been convincingly shown to be a ferroxidase in the fly or even insects. In this work, we provided strong evidence to indicate the existence of a multicopper-oxidase-type ferroxidase in insects; *Drosophila* MCO3 is a ferroxidase, with little laccase and ascorbate oxidase activities; *Drosophila* MCO3-null mutant generated by *CRISPR/Cas9* displayed iron dyshomeostasis but insignificant overall survival phenotypes.

## Results

### Recombinant dMCO3 is associated with potent ferroxidase activity *in vitro*

To test whether dMCO3 has ferroxidase activity, we first tried to express dMCO3 in *E. coli* via intracellular or secretion expression, but neither approach was successful in expressing active dMCO3. We then expressed dMCO3 protein in Sf9 insect cell using the baculovirus expression system. The protein sequence of dMCO3 is predicted to contain a putative signal peptide according to SignalP 4.1 Server (<http://www.cbs.dtu.dk/services/SignalP/>), with a potential cleavage site in between amino acid 51 and 52 from the N-terminal. To accomplish more efficient secreted expression for recombinant protein production, this putative signal peptide was substituted by gp67 signal peptide. The secreted protein was purified from the serum-free medium by Ni-NTA agarose. Purity of the recombinant dMCO3 (about 10 $\mu$ g) was confirmed by SDS-PAGE followed by Coomassie staining (Figure. 1A).

Subsequently, the purified dMCO3 was analyzed for copper content by ICP-MS. Based on the protein concentration of the sample, the purified recombinant dMCO3 was estimated to contain  $2.87 \pm 0.07$  copper atoms/molecule. The holoenzyme of MCO should theoretically contain 4 copper/molecule in the holo form. Less than four copper per protein molecule indicates some of the proteins might be in the apo-protein form or something in between. This also happened to yeast Fet3p, another MCO ferroxidase which when purified was found to contain  $1.5 \pm 0.1$  Cu atoms/molecule (de Silva et al., 1997). Loss of copper could occur during the purification process of dMCO3. Another reason might be our protein is not homogeneous. The prepared dMCO3 was not stable and tended to aggregate, suggesting at least some fraction is not correctly folded. Careful examination of dMCO3 sequence revealed multiple Cys residues, which might reduce folding efficiency during the recombinant expression.

One typical feature of type I copper proteins, as described in another well studied ferroxidase, Fet3p (Hassett et al., 1998), is a 600nm absorbance peak in the UV-visible spectrum. This feature confers them the typical blue color. dMCO3 displayed a similar absorbance peak around 600nm. Addition of ferrous iron resulted in a drop of the signal (Figure. 1B). These results suggest MCO3 is a type 1 copper-containing enzyme, and the particular type I copper is directly involved in the conversion of ferrous iron to ferric iron.

Using ferrous ammonium sulfate (FAS) as a substrate, the ferroxidase activity of dMCO3 was quantitatively ascertained by the absorbance of  $\text{Fe}^{3+}$  at 310nm, which directly reflects the production of  $\text{Fe}^{3+}$  by the catalyzed reaction (Minotti and Ikeda-Saito, 1992). The absorbance readings of purified dMCO3 protein (about 2 $\mu\text{g}$ ) and human ceruloplasmin (about 2 $\mu\text{g}$ ) were kinetically monitored. The results showed that the obtained dMCO3 had more than 50% specific ferroxidase activity than that of human ceruloplasmin (Figure. 1C), indicating dMCO3 is a potent ferroxidase *in vitro*.

In mammals, ferrous iron is transported across the membrane of the cell by ferroportin and then oxidized by hephaestin/ceruloplasmin to ferric iron before being delivered to apo-transferrin. In this process, the ferroxidase activity of hephaestin/ceruloplasmin is critical for the transition of ferrous to ferric iron and subsequent incorporation into apo-transferrin. Likewise, it is reported that yeast Fet3 can also function similarly (de Silva et al., 1997). Addition of human apo-transferrin, which binds the newly formed  $\text{Fe}^{3+}$  from the ferroxidase-catalyzed enzymatic reaction, can speed up the ferroxidation process. Using this method or transferrin loading assay (Johnson et al., 1967; Peng et al., 2015), a strong ferroxidase activity for dMCO3 was also observed; After subtracting the background due to auto-oxidation (which is very low as shown in figure 1C), the recombinant dMCO3 activity was estimated to be 50% of the positive control, ceruloplasmin, while that of the negative control laccase is much lower (Figure. 1D-E). The low activity of laccase is probably a background signal arising from the auto-oxidation of ferrous by oxygen. Using a separately prepared dMCO3 sample, we performed an enzyme concentration vs activity assay. dMCO3-mediated apo-transferrin iron loading is in a linear concentration-dependent manner, and is about 20% of that from ceruloplasmin (Figure. 1F). These results indicate dMCO3 is a potent ferroxidase, and depending on assays and preparations, it has roughly about 25-70% activity of that of human ceruloplasmin.

Azide was reported to have an inhibitory role on the activity of multicopper oxidases due to its interference with type 1 or mononuclear copper sites in the enzymes (Curzon, 1966; Lovstad, 1979). Consistently, the ferroxidase activity of dMCO3 was reduced about 47% by addition of 1mM azide to the reaction buffer, similar to that of human ceruloplasmin (53%) (Figure. 1G, Table 1).

#### **dMCO3 lacks strong laccase or ascorbate oxidase activity**

Depending on substrate specificity, major types of multicopper oxidase include laccases,

ferroxidases and ascorbate oxidases. Having demonstrated a potent ferroxidase activity, we wondered whether dMCO3 could also possibly be associated with laccase or ascorbate oxidase activity. Previously dMCO1 was initially reported to possess ferroxidase activity, and only later found to have very low ferroxidase activity but instead much stronger ascorbate oxidase activity (Peng et al., 2015). We used L-ascobic acid as a substrate for ascorbate oxidase and ABTS (2, 2'-azino-bis (3-ethylbenzothiazoline-6-sulphonic acid) for laccase activity monitoring. Ascorbate Oxidase from *Cucurbita sp.* and Laccase from *Trametes versicolor* were used respectively as the positive controls. The results showed dMCO3 has only very limited ascorbate oxidase or laccase activity (Figure. 2).

#### **dMCO3 expression is developmentally regulated and the protein is likely secreted**

According to the FlyAtlas (<http://flyatlas.org>), *dMCO3* is a low abundance gene expressed in multiple tissues in *Drosophila*. We first analyzed whether the gene expression changes through developmental stages by semi-quantitative PCR. *dMCO3* mRNA has a low but comparably stronger expression at the 1st instar larvae and pupae stages, but very low level in the 2nd-3rd wandering larvae and adult stages (Figure. 3A), when its expression could hardly be detected with 30 cycles PCR reaction.

We generated a homemade mouse polyclonal antiserum against dMCO3. When we used this antibody to stain the dMCO3-overexpressing Sf9 cells, some signals were found on the surface of the cells (Figure. 3Ba). However, when we removed the predicted signal peptide of the protein (Figure. 3C), the signal showed up in the cytosol (Figure. 3Bb). This suggests the antibody is specifically against dMCO3 because by modifying only the potential dMCO3 localization determining sequence, different spatial signals were observed. However, significant *in vivo* expression of dMCO3 was hard to detect with this antibody in the immuno-stained larval cells. Even when overexpressed, no expression was found in most tissues except on the surface of salivary gland cells (Figure. 3C). We suspect that normal expression of dMCO3 may be largely secreted and confined to the extracellular space, making the protein hard to detect even in the overexpressed state. Unfortunately, our antibody does not work on western so we were unable to check dMCO3 in the hemolymph.

To confirm the extracellular localization of dMCO3, we over-expressed a C-terminal His-tagged dMCO3 in Sf9 cells, with its own N-terminal sequence, and checked the expression with Western Blot using the His-tag antibody. dMCO3 indeed appeared in the cell-free culture. When we removed partially the predicted signal peptide (the potential transmembrane domain), no dMCO3 protein was found in the media (Figure. 3E), suggesting that when expressed in sf9 cells the potential secretion signal indeed led dMCO3 secreted.

#### **dMCO3 is involved in iron homeostasis**

The above biochemical analysis indicated that dMCO3 is a ferroxidase *in vitro*. We then studied whether *dMCO3* is involved in iron export, as both in mammals and yeast the main function of multicopper ferroxidase is to facilitate iron transport across the membrane.

To explore the *in vivo* physiological functions of *dMCO3* in *Drosophila*, a null mutant is generated using the CRISPR-CAS9 system (Ren et al., 2013; Ren et al., 2014) (Figure. 4A). Reverse-transcription PCR (RT-PCR) analysis revealed that the gene is truly removed (Figure. 4B). To ascertain the role of *dMCO3* in iron metabolism, we measured total iron content of the whole fly and head using inductively coupled plasma-mass spectrometry (ICP-MS). The results show that *dMCO3* knockout flies displayed approximately 30% and 100% higher total iron content when raised on normal food and 5mM iron-supplemented food respectively than the wild-type flies (Figure. 4C-D). In the head of *dMCO3* knockout flies, the iron level had 20% increase compared with wild type flies (Figure. 4E). When *dMCO3* was overexpressed, the total iron content decreased about 20% on iron food (Figure. 4D). Consistently, real-time quantitative PCR result showed that the iron-responsive *Malvolio* (*Mvl*), a potential fly orthologue of the mammalian iron importer DMT1, was also downregulated in the head of *dMCO3*-null flies (Figure. 4F). These results indicate that *dMCO3* functions to modulate iron homeostasis and the absence of *dMCO3* leads to iron accumulation in the head.

Previously it was reported that one *Mvl* mutant allele, *MCO3*<sup>C359</sup>, accumulated more iron in the iron cell region of gut. We stained the gut from *dMCO3*-null mutant fly larvae for ferric iron, and consistently we found stronger signals in the iron cell region. Under 5mM iron food, the signal at the anterior midgut of *dMCO3* knockout flies also became further increased (Figure. 4G). Ferrozine based assay indicated that *dMCO3*-null mutant guts accumulated about 2/3 more iron than those of the control flies (Figure. 4H).

We further analyzed how genes involved in iron homeostasis might respond to the loss of *dMCO3* in the gut, such as *Mvl*, *dZIP13* and ferritin genes (Missirlis et al., 2007; Tang and Zhou, 2013a; Xiao et al., 2014). Our real-time qRT-PCR result showed that the mRNA level of *Mvl* decreased on both normal food and iron-supplemented food, while *dZIP13* increased under both food conditions for *dMCO3* knockout flies (Figure. 4I). Ferritin expression was however not much altered. The results are consistent with a decrease in iron import and an increase in export through the secretory pathway, suggesting that iron is accumulated in the gut of *dMCO3* knockout flies, which may result a compensatory expression change of other genes involved in iron metabolism.

Homozygous *dMCO3* mutant flies were viable and displayed no obvious external phenotypes under normal conditions (Figure. 5A). To examine whether the knockout flies are susceptible to iron-stress, first instar larvae were raised to adulthood on a range of iron-chelated and iron-supplemented media. Homozygous mutant larvae still displayed no obvious survival defects (such as eclosion) on this low-iron or high-iron media (Figure. 5B), suggesting *dMCO3* is not essential under normal or iron-stressed conditions. This lack of obvious overt phenotype suggests although *dMCO3* is involved in iron homeostasis in the fly, the extent of influence is not great enough to cause obvious external abnormality. The adverse physiological effects caused by *dMCO3* removal might be largely bypassed by other compensatory mechanisms as analyzed above.

## Discussion

The oxidation of ferrous iron to ferric iron, as mediated by multicopper ferroxidases, is an essential step in iron transport for mammals and yeast. However, whether there exists a similar gene or biological process in *Drosophila* remains unknown until now. Here, we identified *dMCO3* as a *Drosophila* ferroxidase. Specifically, we found *dMCO3* has potent ferroxidase activity but little laccase or ascorbate oxidase activity *in vitro* using recombinant *dMCO3* protein. Further analyses indicate that *in vivo* *dMCO3* affects iron homeostasis, and is possibly a secreted protein. In this sense, *dMCO3* is reminiscent of the serum form of ceruloplasmin in mammals.

In mammals, mutations in hephaestin and ceruloplasmin result respectively in overall iron deficiency/anemia and iron accumulation in several tissues (Chen et al., 2004; Jeong and David, 2006; Jiang et al., 2015). However, at the cellular level, both multicopper ferroxidases are involved

in cellular iron efflux (Chen et al., 2009; Jeong and David, 2003). Interestingly in this work, *dMCO3* loss also results increased iron content, implying that a similar process might exist in the fly. Notably, in the fly, iron export is mainly carried out through ferritin secretion. It has been shown that ferritin is the key to *Drosophila* dietary iron absorption (Tang and Zhou, 2013a). *Fanis Missirlis et.al* reported that the ferroxidase activity of Fer1HCH is essential for the fly survival (Missirlis et al., 2007), a conclusion further supported by the study that expression of mutant ferroxidase Fer1HCH cannot rescue the lethality of the Fer1HCH mutant (Gonzalez-Morales et al., 2015). When dZIP13 expression is suppressed, iron loading is much reduced in ferritin, causing a similar iron dyshomeostasis phenotype as ferritin down-regulation (Xiao et al., 2014). A proposed scenario is that *Drosophila* ZIP13 exports iron to the ER/Golgi, where iron is oxidized and loaded to ferritin. The iron-loaded ferritin then carries with it iron to deliver to other parts of the body (Tang and Zhou, 2013b). The lack of serious phenotype of *dMCO3*-null flies, therefore, suggests to us that although a similar multicopper/ferroportin system might exist in the fly, the presence of the predominant dZIP13-ferritin iron export system may make it physiologically less significant.

In *Drosophila*, whether there exists a functional homolog of ferroportin is still unclear. Database search reveals no annotated proteins with significant similarity to mammalian ferroportin. If there is really one ferroportin counterpart in the fly, then the sequence might be too divergent from ferroportin. If on the other hand there is none, it would be hard to conceive how ferroxidase such as *dMCO3* might work. The observation that *dMCO3*-null flies displayed iron homeostasis implicates the existence of a similarly functional ferroportin counterpart in the fly. Additionally baffling is that no obvious MCO3 exists in some other insects such as *Anopheles gambiae*; there are only three potential MCOs in the mosquito, and the mosquito MCO3 appears quite different from fly MCO3 (i.e., they are not orthologous). These observations suggest that the multicopper/ferroportin iron efflux process might indeed become dispensable or even get lost in some insects during evolution, considering that the major iron export process in this evolution tree branch could be replaced by the ZIP13-ferritin axis along the secretion pathway.

## Methods and Materials

### *dMCO3* expression in insect cell

A cDNA fragment encoding amino acid (AA) 52-677 of dMCO3, which excludes the signal peptide (AA 1-51) as predicted by SignalP 4.1 Server, was amplified and cloned into pFast-Bac-Dual vector (Invitrogen, Carlsbad, CA, USA) for recombinant baculovirus preparation. To accomplish more efficient secreted expression, a GP67 signal peptide was added at the N-terminal in-frame with dMCO3. A 6Xhis tag was fused to the C-terminal of dMCO3. The recombinant baculovirus was transfected to Sf9 cells and the secreted enzyme was purified by Ni-NTA Agarose (Qiagen, Hilden, Germany).

#### **UV-visible spectrum assay of dMCO3**

The UV-visible spectrum of dMCO3 was detected from 250nm to 800nm by Spectrophotometry (Multiskan Go, Thermo Electron Corp, Waltham, MA, USA). To study iron influence, 80 $\mu$ M final concentration of freshly made ferrous ammonium sulfate was added to the dMCO3 solution (3.3mg/ml, in 100mM MES, 150mM NaCl, pH5.8) to analyze possible spectrum change.

#### **Ferroxidase activity assay**

Ferroxidase activity measurement was performed as described previously (Wong et al., 2014). Briefly, the enzymatic reaction was performed in a 96 well microplate. 2 $\mu$ g protein was added into reaction buffer containing 0.1M HEPES, pH6.5. 0.1mM freshly made ferrous ammonium sulfate was used as the substrate. Absorbance at 310nm, reflecting the production of ferric iron, was kinetically monitored over one hour at intervals of 30s at room temperature. Human ceruloplasmin (BioVision, #4096-1000, Milpitas, USA) was used as a positive control. For transferrin-loading-based ferroxidase activity assay, the reaction was performed in a 96 well microplate in 0.1M MES buffer, pH6.5. Reactions (100 $\mu$ l) contained about 8 $\mu$ g enzyme, 780 $\mu$ g Apo-Transferrin (Sigma, #T1147-100MG, St. Louis, MO, USA), 0.1mM ferrous ammonium sulfate. The formation of Fe<sup>3+</sup>-transferrin complex was determined by measuring absorbance at 460nm, using a molar extinction coefficient of 2500 M<sup>-1</sup> cm<sup>-1</sup> (Peng et al., 2015).

#### **Laccase and ascorbate oxidase activity assays**

Laccase and ascorbate oxidase activity assays were performed in 0.1M MES buffer, pH6.5. The absorbance is monitored respectively with the laccase at 420nm and ascorbate oxidase at 275nm, at intervals of 30s until the reaction reaches plateau (Peng et al., 2015). The reactions of both assays were performed in a total volume of 200 $\mu$ l including equal amounts of positive control and dMCO3 (about 5 $\mu$ g), 0.5mM ABTS (2,2'-Azino-bis (3-ethylbenzothiazoline-6-sulfonic acid)

diammonium salt, Sigma, #A1888, St. Louis, MO, USA) for laccase, 0.5mM L-ascorbic acid (Sigma, #A0278, St. Louis, MO, USA) for ascorbate oxidase. Laccase from *Trametes versicolor* (Sigma, #38429, St. Louis, MO, USA) and Ascorbate Oxidase from *Cucurbita sp.* (Sigma, #A0157-100UN, St. Louis, MO, USA) were used as positive controls. Molar extinction coefficients for ascorbate oxidase activity assay and that of laccase are 12,000 M<sup>-1</sup> cm<sup>-1</sup> and 36,000 M<sup>-1</sup> cm<sup>-1</sup> respectively.

#### **dMCO3-null mutant generation**

The dMCO3-null mutant was prepared as reported previously (Ren et al., 2013). The two sgRNA (sgRNA1: 5'-ATCGAGTGGCCAGTTGCCCG-3', sgRNA2: 5'-GGCGGTGCTGAAGATCGGTG-3') plasmids were injected into *y[1] sc[1] v[1] P{y[+t7.7]=nos-phiC31\int.NLS}X; P{y[+t7.7]=CaryP}attP40* (the host control) fly embryos followed by screening for vermilion+ marker present in the plasmid. The transgenic flies were then crossed to nos-Cas9 flies with the same genetic background. dMCO3 knockout was screened by PCR using genomic DNA. Two pairs of primers were used to validate the knockout flies. primer1# (F: 5'-TCTGTATGCTTCATTGCGAGCTC-3', R: 5'-ACTGGAAGTTGAGGAGGTTACAGATA-3') and primer2# (F: 5'-TCTCTACCAGGACGATAGATACTTC-3' R: 5'-TGCTTCAACATGGCAATGATATAGC-3').

#### **Metal content assay by ICP-MS**

Equal numbers of mixed male and female 5-day-old adult flies (30 in total per group for head and 6 for whole body) were collected. For flies raised on iron-supplemented diet, they were transferred to normal diet for 24 h to clear the high-iron food from the gut lumen before metal content analysis. Samples were digested in 0.3ml nitric acid, brought to 6ml in volume and then subjected to metal content analysis by inductively coupled plasma-mass spectrometry (ICP-MS) XII (Thermo Electron Corp, Waltham, MA, USA) at Peking University Health Science Center (Beijing, China).

#### **Ferrozine-based iron content assay**

To estimate whether dMCO3 knockout can alter the iron level in the gut, we used a Ferrozine-based assay as described previously (Lang et al., 2012). Fly gut were dissected in PBS buffer and lysed in 1% NP-40 Buffer. Samples were centrifuged to remove insoluble material. The iron concentration was calculated based on a molar extinct ion coefficient of the iron–Ferrozine complex of 27,900M<sup>-1</sup>cm<sup>-1</sup>(Carter, 1971).

#### **Preparation of anti-dMCO3 polyclonal antiserum**

Mouse polyclonal antibodies were raised against recombinant dMCO3 expressed in *E. coli*. Briefly,

a cDNA fragment encoding AA 52-677 was amplified and cloned into pGEX-6p-1(GE Healthcare). A 10×histidine tag was added to the N-terminal for Ni-NTA Agarose (Qiagen,Hilden,Germany) purification. The recombinant protein, in the form of inclusion body, was solubilized with urea and purified. The purified protein was dialyzed for partial refolding and subsequently injected into mice for antibody generation by Proteintech Group (Wuhan, China). The anti-serum was further purified by Protein A Agarose (Sigma, St. Louis, MO, USA) for use. Specificity of the antibody was checked initially by comparing the staining signals from dMCO3 overexpression and knockout larvae, and later further validated by staining dMCO3 overexpressed in sf9 cells. See the text for more details.

#### **Eclosion and longevity assays**

To explore *in vivo* functions of *dMCO3* in the fly, we reared the progeny on food containing different metals or metal chelators. The concentrations of supplemented metals or metal chelators used were as follows: 5mM Ferric ammonium citrate (FAC), 0.2mM Bathophenanthrolinedisulfonic acid disodium (BPS) (Sigma, St. Louis, MO, USA). Each vial contained about 50 progenies. The total number adult flies were counted after eclosion. For longevity assay, 3-day-old adult males were collected and placed in a food vial with 20 flies each at 29°C with 60% humidity under a 12-hr light–dark cycle. Food vials were changed every 3 days, and dead flies were counted. At least 4 replicates were conducted for each group. Data were calculated as described previously (Xiao et al., 2014).

#### **RNA extraction and real-time RT-PCR**

To analyze temporal expression profile of *dMCO3*, fly samples at different developmental stages were collected for RNA extraction. Total RNA was extracted with TRIzol Reagent (Invitrogen, Carlsbad, CA, USA). cDNA was reverse transcribed from 1µg total RNA with TransScript Reverse Transcriptase (TransGen Biotech Co., Beijing, China). Real-time RT-PCR was performed as described previously (Wang et al., 2009). The primes for *RP49*, *MCO3* and *Mvl* were described previously (Bettendi et al., 2011). dZIP13-F: 5'-ATTCCCGCTGATCATCATTC-3'; dZIP13-R: 5'-GCAGGGATGGGTGACTAGAA-3'

#### **Immunostaining**

Sf9 cells were maintained in Sf-900™ III SFM (Gibco,Gaithersburg, MD, USA) at 27°C. 24hrs after infection with baculovirus containing dMCO3, cells were fixed, taken pictures after staining with MCO3 antibody. For dMCO3 staining in fly samples, salivary glands were dissected, fixed, stained, and mounted as described previously (Pastor-Pareja and Xu, 2011). Goat anti-mouse IgG

conjugated to FITC (ZhongshanGoldenbridge Biotechnology, Beijing, China) (1:500) was used as the secondary antibody. For DAPI staining, samples were incubated in 50ng/ml DAPI for 10 min. Slides were mounted with 50% glycerol/PBS. Confocal images were taken with a Zeiss LSM710 Meta confocal microscope.

### **Western Blot**

The baculovirus infected supernant were collected and separated on 12% SDS-PAGE, and transferred to PVDF membranes (Millipore, Watford, UK). Anti-His Mouse mAb (1:4000) was obtained from Abmart (Shanghai, China). HRP-linked Anti-Mouse IgG (1:2000) was from Cell Signaling Technology (Danvers, MA, USA). Signals were detected with ECL method.

### **Statistical analysis**

All statistical analyses were performed using Prism 6.0 software (GraphPad, La Jolla, CA). Data were analyzed by Student's t-test between groups, and while multiple groups were compared ANOVA was used. Statistical results were presented as means  $\pm$  SEM. Asterisks indicate critical levels of significance (\* $p$ <0.05, \*\* $p$ <0.01, and \*\*\* $p$ <0.001).

### **Acknowledgement**

We greatly appreciate the fly stocks and service from Tsinghua Fly Center (Beijing, China). This work was supported by grants from the National Science Foundation of China (31123004) and the National Basic Research Program of China (2013CB910700).

### **Author contributions**

Bing Zhou conceived and guided the project and reviewed the manuscript. Xudong Wang planned and carried out experiments and analyzed the resulting data and wrote the manuscript. Sai Yin performed the tissue staining and iron staining. Zhihao Yang assisted with *dMCO3 KO* preparation.

### **Conflict of interests**

The authors declare that they have no conflict of interests.

## References

- Andersson, K. K., Vassort, C., Brennan, B. A., Que, L., Jr., Haavik, J., Flatmark, T., Gros, F., and Thibault, J. (1992). Purification and characterization of the blue-green rat pheochromocytoma (PC12) tyrosine hydroxylase with a dopamine-Fe(III) complex. Reversal of the endogenous feedback inhibition by phosphorylation of serine-40. *Biochem J* 284 ( Pt 3), 687-695.
- Askwith, C., Eide, D., Van Ho, A., Bernard, P. S., Li, L., Davis-Kaplan, S., Sipe, D. M., and Kaplan, J. (1994). The FET3 gene of *S. cerevisiae* encodes a multicopper oxidase required for ferrous iron uptake. *Cell* 76, 403-410.
- Bettedi, L., Aslam, M. F., Szular, J., Mandilaras, K., and Missirlis, F. (2011). Iron depletion in the intestines of Malvolio mutant flies does not occur in the absence of a multicopper oxidase. *J Exp Biol* 214, 971-978.
- Bou-Abdallah, F., Zhao, G., Biasiotto, G., Poli, M., Arosio, P., and Chasteen, N. D. (2008). Facilitated diffusion of iron(II) and dioxygen substrates into human H-chain ferritin. A fluorescence and absorbance study employing the ferroxidase center substitution Y34W. *J Am Chem Soc* 130, 17801-17811.
- Calap-Quintana, P., Gonzalez-Fernandez, J., Sebastia-Ortega, N., Llorens, J. V., and Molto, M. D. (2017). *Drosophila melanogaster* Models of Metal-Related Human Diseases and Metal Toxicity. *Int J Mol Sci* 18.
- Carter, P. (1971). Spectrophotometric determination of serum iron at the submicrogram level with a new reagent (ferrozine). *Anal Biochem* 40, 450-458.
- Charlesworth, A., Georgieva, T., Gospodov, I., Law, J. H., Dunkov, B. C., Ralcheva, N., Barillas-Mury, C., Ralchev, K., and Kafatos, F. C. (1997). Isolation and properties of *Drosophila melanogaster* ferritin--molecular cloning of a cDNA that encodes one subunit, and localization of the gene on the third chromosome. *Eur J Biochem* 247, 470-475.
- Chen, H., Attieh, Z. K., Dang, T., Huang, G., van der Hee, R. M., and Vulpe, C. (2009). Decreased hephaestin expression and activity leads to decreased iron efflux from differentiated Caco2 cells. *J Cell Biochem* 107, 803-808.
- Chen, H., Attieh, Z. K., Su, T., Syed, B. A., Gao, H., Alaeddine, R. M., Fox, T. C., Usta, J., Naylor, C. E., Evans, R. W., *et al.* (2004). Hephaestin is a ferroxidase that maintains partial activity in sex-linked anemia mice. *Blood* 103, 3933-3939.
- Clark, D. V. (1994). Molecular and genetic analyses of *Drosophila* Prat, which encodes the first enzyme

- of de novo purine biosynthesis. *Genetics* 136, 547-557.
- Curzon, G. (1966). The inhibition of caeruloplasmin by azide. *Biochem J* 100, 295-302.
- de Silva, D., Davis-Kaplan, S., Fergestad, J., and Kaplan, J. (1997). Purification and characterization of Fet3 protein, a yeast homologue of ceruloplasmin. *J Biol Chem* 272, 14208-14213.
- Dittmer, N. T., and Kanost, M. R. (2010). Insect multicopper oxidases: diversity, properties, and physiological roles. *Insect Biochem Mol Biol* 40, 179-188.
- Folwell, J. L., Barton, C. H., and Shepherd, D. (2006). Immunolocalisation of the *D. melanogaster* Nramp homologue Malvolio to gut and Malpighian tubules provides evidence that Malvolio and Nramp2 are orthologous. *J Exp Biol* 209, 1988-1995.
- Fox, P. L. (2003). The copper-iron chronicles: the story of an intimate relationship. *Biometals* 16, 9-40.
- Gonzalez-Morales, N., Mendoza-Ortiz, M. A., Blowes, L. M., Missirlis, F., and Riesgo-Escovar, J. R. (2015). Ferritin Is Required in Multiple Tissues during *Drosophila melanogaster* Development. *PLoS One* 10, e0133499.
- Harris, Z. L., Durley, A. P., Man, T. K., and Gitlin, J. D. (1999). Targeted gene disruption reveals an essential role for ceruloplasmin in cellular iron efflux. *Proc Natl Acad Sci U S A* 96, 10812-10817.
- Hassett, R. F., Yuan, D. S., and Kosman, D. J. (1998). Spectral and kinetic properties of the Fet3 protein from *Saccharomyces cerevisiae*, a multinuclear copper ferroxidase enzyme. *J Biol Chem* 273, 23274-23282.
- Jeong, S. Y., and David, S. (2003). Glycosylphosphatidylinositol-anchored ceruloplasmin is required for iron efflux from cells in the central nervous system. *J Biol Chem* 278, 27144-27148.
- Jeong, S. Y., and David, S. (2006). Age-related changes in iron homeostasis and cell death in the cerebellum of ceruloplasmin-deficient mice. *J Neurosci* 26, 9810-9819.
- Jiang, R., Hua, C., Wan, Y., Jiang, B., Hu, H., Zheng, J., Fuqua, B. K., Dunaief, J. L., Anderson, G. J., David, S., *et al.* (2015). Hephaestin and ceruloplasmin play distinct but interrelated roles in iron homeostasis in mouse brain. *J Nutr* 145, 1003-1009.
- Johnson, D. A., Osaki, S., and Frieden, E. (1967). A micromethod for the determination of ferroxidase (ceruloplasmin) in human serums. *Clin Chem* 13, 142-150.
- Kosman, D. J. (2010). Redox cycling in iron uptake, efflux, and trafficking. *J Biol Chem* 285, 26729-26735.
- Lang, M., Braun, C. L., Kanost, M. R., and Gorman, M. J. (2012). Multicopper oxidase-1 is a ferroxidase essential for iron homeostasis in *Drosophila melanogaster*. *Proc Natl Acad Sci U S A* 109, 13337-13342.

- Li, S. (2010). Identification of iron-loaded ferritin as an essential mitogen for cell proliferation and postembryonic development in *Drosophila*. *Cell Res* 20, 1148-1157.
- Locke, M., and Leung, H. (1984). The induction and distribution of an insect ferritin--a new function for the endoplasmic reticulum. *Tissue Cell* 16, 739-766.
- Lovstad, R. A. (1979). Activating effect of copper ions on the interaction of ceruloplasmin with catecholamines. *Gen Pharmacol* 10, 147-151.
- Mandilaras, K., Pathmanathan, T., and Missirlis, F. (2013). Iron absorption in *Drosophila melanogaster*. *Nutrients* 5, 1622-1647.
- Minotti, G., and Ikeda-Saito, M. (1992). Fe(II) oxidation and Fe(III) incorporation by the M(r) 66,000 microsomal iron protein that stimulates NADPH oxidation. *J Biol Chem* 267, 7611-7614.
- Missirlis, F., Kosmidis, S., Brody, T., Mavrakis, M., Holmberg, S., Odenwald, W. F., Skoulakis, E. M., and Rouault, T. A. (2007). Homeostatic mechanisms for iron storage revealed by genetic manipulations and live imaging of *Drosophila* ferritin. *Genetics* 177, 89-100.
- Nichol, H., Law, J. H., and Winzerling, J. J. (2002). Iron metabolism in insects. *Annu Rev Entomol* 47, 535-559.
- Pastor-Pareja, J. C., and Xu, T. (2011). Shaping cells and organs in *Drosophila* by opposing roles of fat body-secreted Collagen IV and perlecan. *Dev Cell* 21, 245-256.
- Peng, Z., Dittmer, N. T., Lang, M., Brummett, L. M., Braun, C. L., Davis, L. C., Kanost, M. R., and Gorman, M. J. (2015). Multicopper oxidase-1 orthologs from diverse insect species have ascorbate oxidase activity. *Insect Biochem Mol Biol* 59, 58-71.
- Ren, X., Sun, J., Housden, B. E., Hu, Y., Roesel, C., Lin, S., Liu, L. P., Yang, Z., Mao, D., Sun, L., *et al.* (2013). Optimized gene editing technology for *Drosophila melanogaster* using germ line-specific Cas9. *Proc Natl Acad Sci U S A* 110, 19012-19017.
- Ren, X., Yang, Z., Xu, J., Sun, J., Mao, D., Hu, Y., Yang, S. J., Qiao, H. H., Wang, X., Hu, Q., *et al.* (2014). Enhanced specificity and efficiency of the CRISPR/Cas9 system with optimized sgRNA parameters in *Drosophila*. *Cell Rep* 9, 1151-1162.
- Sheftel, A. D., Mason, A. B., and Ponka, P. (2012). The long history of iron in the Universe and in health and disease. *Biochim Biophys Acta* 1820, 161-187.
- Stearman, R., Yuan, D. S., Yamaguchi-Iwai, Y., Klausner, R. D., and Dancis, A. (1996). A permease-oxidase complex involved in high-affinity iron uptake in yeast. *Science* 271, 1552-1557.

Tang, X., and Zhou, B. (2013a). Ferritin is the key to dietary iron absorption and tissue iron detoxification in *Drosophila melanogaster*. *FASEB J* 27, 288-298.

Tang, X., and Zhou, B. (2013b). Iron homeostasis in insects: Insights from *Drosophila* studies. *IUBMB Life* 65, 863-872.

Vulpe, C. D., Kuo, Y. M., Murphy, T. L., Cowley, L., Askwith, C., Libina, N., Gitschier, J., and Anderson, G. J. (1999). Hephaestin, a ceruloplasmin homologue implicated in intestinal iron transport, is defective in the *sla* mouse. *Nat Genet* 21, 195-199.

Wang, X., Wu, Y., and Zhou, B. (2009). Dietary zinc absorption is mediated by ZnT1 in *Drosophila melanogaster*. *FASEB J* 23, 2650-2661.

Warburg, O. (1925). Iron, the Oxygen-Carrier of Respiration-Ferment. *Science* 61, 575-582.

Wong, B. X., Ayton, S., Lam, L. Q., Lei, P., Adlard, P. A., Bush, A. I., and Duce, J. A. (2014). A comparison of ceruloplasmin to biological polyanions in promoting the oxidation of Fe(2+) under physiologically relevant conditions. *Biochim Biophys Acta* 1840, 3299-3310.

Xiao, G., Wan, Z., Fan, Q., Tang, X., and Zhou, B. (2014). The metal transporter ZIP13 supplies iron into the secretory pathway in *Drosophila melanogaster*. *Elife* 3, e03191.

## Figure legends

### Figure 1. dMCO3 has strong ferroxidase activity *in vitro*.

A Coomassie staining of purified dMCO3. BSA was used to quantify the concentration of dMCO3. 5µl and 10µl of the purified of recombinant dMCO3 were estimated respectively to be around 2 and 4µg.

B UV-visible spectrum of dMCO3. The spectra were detected at room temperature in buffer with 100µM MES, 200mM NaCl, pH5.8. The concentration of dMCO3 was 3.3mg/ml. 80µM freshly made ferrous ammonium sulfate (FAS) was added to monitor the spectrum change at 600nm of dMCO3.

C Kinetics of dMCO3 ferroxidase activity. Absorbance at 310nm measures conversion of Fe<sup>2+</sup> to Fe<sup>3+</sup>. The reaction was performed at room temperature in 0.1M HEPES, pH6.5 with 0.1mM freshly made ferrous ammonium sulfate (FAS). Human ceruloplasmin was used as the positive control. NC refers to the blank buffer control containing ferrous ammonium sulfate (FAS).

D-E dMCO3 ferroxidase activity measurement by transferrin loading assay. The assay was performed in 0.1M MES, pH6.5 containing 780µg apo-Transferrin at room temperature. The formation of Fe<sup>3+</sup>-transferrin was monitored at 460nm. The buffer control without enzyme or the background, which is very low (as shown in figure 1C), was already subtracted from the results. Laccase from *Trametes versicolor* was used as the negative control.

F Incorporation of Fe (II) into Apo-transferrin by dMCO3 and ceruloplasmin. Reactions were carried out in 100µl volume containing 780µg Apo-transferrin, 100µM ferrous ammonium sulfate and different amounts of dMCO3. The Fe (III)-transferrin complex was monitored at 460 nm. Shown results are background-subtracted.

G Effect of azide on dMCO3 ferroxidase and ceruloplasmin activity. The assay was performed according to transferrin loading assay with the addition of 1mM azide. Azide led to about 47% reduction of dMCO3 ferroxidase activity and 53% of ceruloplasmin activity respectively. The buffer control without enzyme acts as the background control, and the results are background-subtracted.

### Figure 2. dMCO3 has no strong ascorbate oxidase and laccase activities.

A Ascorbate oxidase activity of dMCO3 was monitored at 275nm with L-ascorbic acid (500µM) as the substrate. Ascorbate Oxidase from *Cucurbita sp.* was used as the positive control. The buffer control without enzyme was subtracted from the results.

B Laccase activity of dMCO3 was performed at 420nm in the presence of ABTS (500µM). Laccase from *Trametes versicolor* was used as the positive control. Background was subtracted from the results. The two assays (A-B) were both measured in 0.1M MES, pH6.5 buffer

### Figure 3. dMCO3 is likely predominantly secreted.

A Real-time RT-PCR analysis of dMCO3 at different developmental stages. Abbreviations: L1, 1st instar larvae; L2, 2nd instar larvae; L3, 3rd instar larvae; Means±SD are shown. Data were normalized to *rp49* expression.

B (a). The localization of dMCO3 in dMCO3-expressing Sf9 cell. DAPI was used to mark the nucleus. (b). Confocal images of dMCO3\* (removing the potential secretion signal and the transmembrane helix). DAPI was used to mark the nucleus. Scale bars: 20µm.

C Sequence of dMCO3 protein. The underlined segment is the predicted signal peptide. A potential transmembrane sequence is highlighted in red.

D Cryosections of larval salivary glands of control (normal), *dMCO3* knockout (*dMCO3 KO*) and *dMCO3* over-expression (*Da>UAS-dMCO3*) strains were immunostained with Protein G-purified *dMCO3* polyclonal antiserum. Scale bars: 50 $\mu$ m. The immunofluorescence staining showed some *dMCO3* was present on the cell membrane of salivary gland cells. Scale bars: 50 $\mu$ m.

E Western Blot analysis of *dMCO3* in the supernatant of sf9 cell. *dMCO3\** is a *dMCO3* mutant removing partially the predicted signal peptide. NC, blank sf9 cell supernatant as the negative control. PC, purified *dMCO3* protein as the positive control. Roughly equal total protein was loaded for each lane except for the PC control. Coomassie Brilliant Blue (CBB) staining was performed in parallel for the loaded supernatants.

**Figure 4. *dMCO3* is involved in iron homeostasis.**

A Schematic diagram of generating *dMCO3*-null flies by CRISPR-CAS9. The genomic region between sgRNA1 and sgRNA2 was deleted. Two pairs of primers, primer1# and primer2#, were later used to validate *dMCO3* knockout.

B Results of validation for the *dMCO3*-null mutant using the two pairs of testing primers. Primer1# is expected to amplify a 0.5 kb DNA fragment from the mutant and a 2.5kb fragment from the control. However, with a PCR extension time of 50 seconds in our assays, this 2.5kb band normally is not amplified from the control.

C-D Metal content analysis by ICP-MS in the adult fly reared on normal food (C) food supplemented with 5mM iron (D). The level of iron increased in the whole body on both normal and iron food for *dMCO3* knockout flies whereas decreased in the ubiquitously overexpressed *dMCO3* flies. Other metals including Zn, Cu, Mn did not obviously change. Metal content results are presented as means $\pm$ SEM; n = 3. \*p<0.05, \*\*p<0.01; two-tailed Student's *t* test. For *dMCO3* over expression, Ubiquitous expressed *Da-Gal4* was crossed to *UAS-dMCO3/Cyo* and non-*Cyo* progeny were selected for further experiments. The control strain was the host strain used for injection (see Methods and Materials)

E Iron content is also increased in the head of *dMCO3* knockout flies. Metal content results are presented as means $\pm$ SEM; n = 3. \*p<0.05, \*\*p<0.01; two-tailed Student's *t* test.

F Real-time qPCR analysis of *Mvl* in the head of *dMCO3*-null mutant. Knockout of *dMCO3* resulted in a decrease in *Mvl* mRNA level in the head. Data were normalized to *rp49* expression. Data are from three biological replicates. Means $\pm$ SD are shown. Differences in expression were assessed by performing an unpaired *t* test (\*p<0.05, \*\*p<0.01, \*\*\*p<0.001).

G Staining of ferric iron in the larval gut reared on normal food (NF) and food with 5mM iron (ammonium ferric citrate, FAC) supplement. Iron cell region was more intensely stained in the *dMCO3* knockout. Anterior midgut staining appeared in the presence of iron supplementation, and it was also stronger in the *dMCO3* knockout.

H Larval gut iron content assayed by Ferrozine. *dMCO3* knockout led to more iron accumulated in the gut. Metal content results are presented as means $\pm$ SEM; n = 3. \*p<0.05, \*\*p<0.01; two-tailed Student's *t* test.

I Real-time qPCR analysis of *Mvl* and *dZip13* in the larval gut of *dMCO3* knockout reared on normal food and 5mM iron supplemented food. Knockout of *dMCO3* resulted in a decrease in *Mvl* mRNA level and increase in *dZip13* mRNA level in the gut. Data are normalized to *rp49* expression and are from three biological replicates. Means $\pm$ SD are shown. Differences in expression are assessed by performing an unpaired *t* test (\*p<0.05, \*\*p<0.01, \*\*\*p<0.001).

**Figure 5. *dMCO3* knockout had little overt effect on lifespan and eclosion in *D.melanogaster*.**

A Longevity analysis of *dMCO3* mutant at 29°C. Control was the injection strain (see Methods and Materials).

B Eclosion rate of *dMCO3* mutant on iron-regulated food at 25°C. No significant changes were observed.

ACCEPTED MANUSCRIPT

**Table 1. Azide has an inhibitory effect on dMCO3 ferroxidase activity**

Condition	V( $\mu$ M/min)	Percent activity (%)
Ceruloplasmin	3.2	100
Ceruloplasmin+1mM NaN <sub>3</sub>	1.5	47
dMCO3	1.5	100
dMCO3+1mM NaN <sub>3</sub>	0.8	53

ACCEPTED MANUSCRIPT

---

**Highlights**

1. *Drosophila* MCO3(dMCO3) is associated with potent *in vitro* ferroxidase activity.
2. dMCO3 lacks significant laccase and ascorbate oxidase activities.
3. *dMCO3* deletion results in altered iron metabolism.
4. *dMCO3* mutant has no significant survival defects.

ACCEPTED MANUSCRIPT

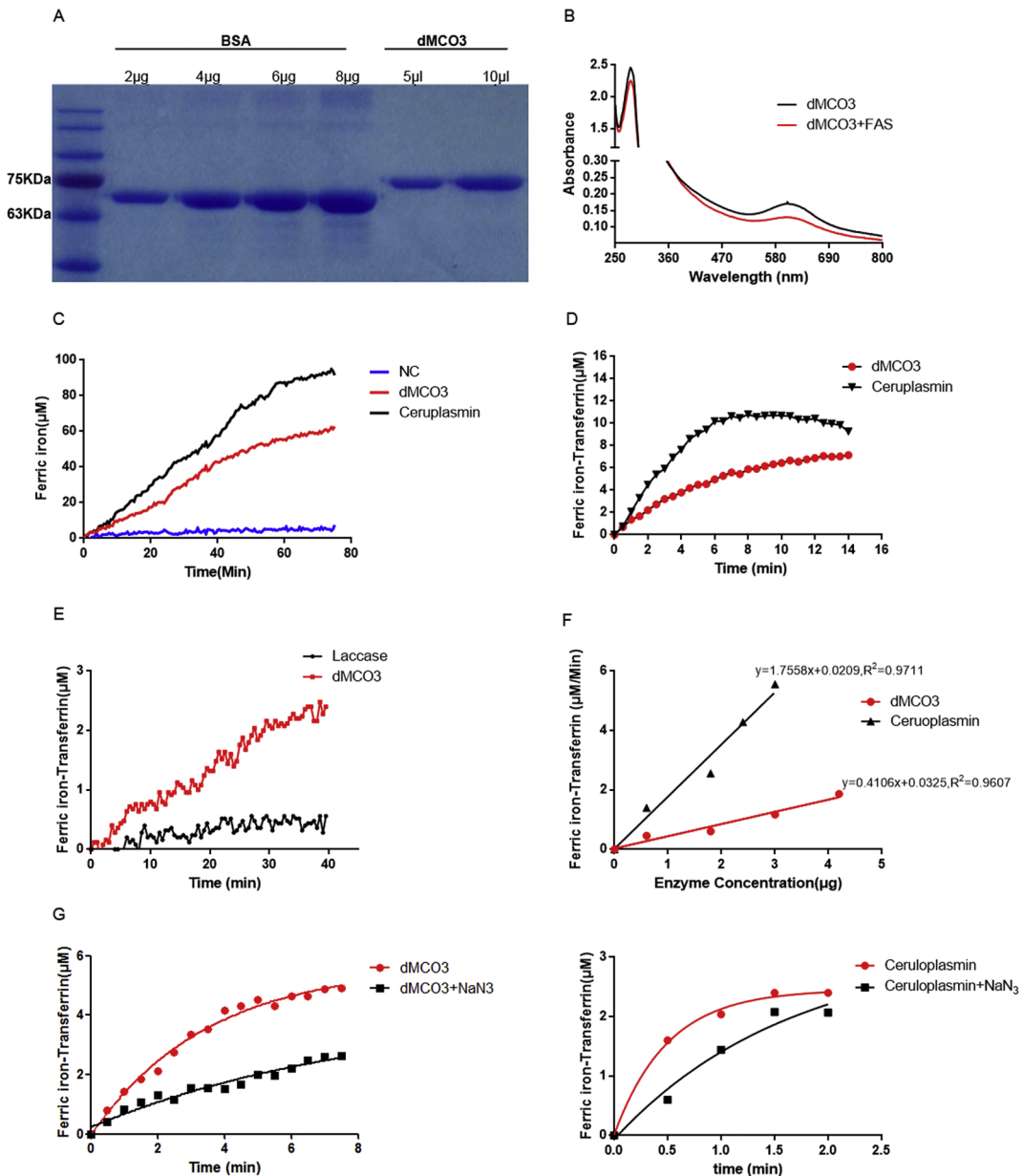


Figure 1

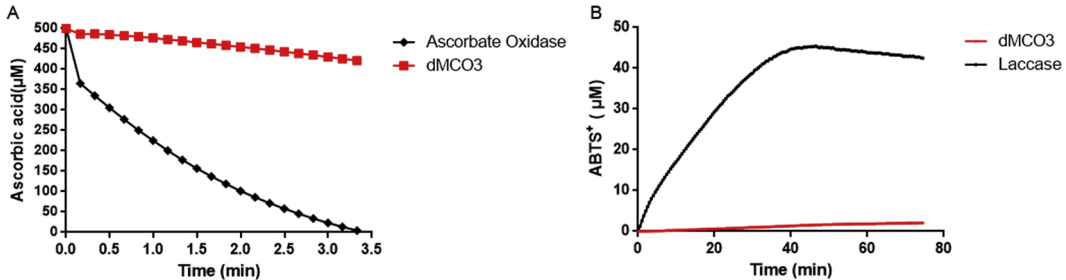
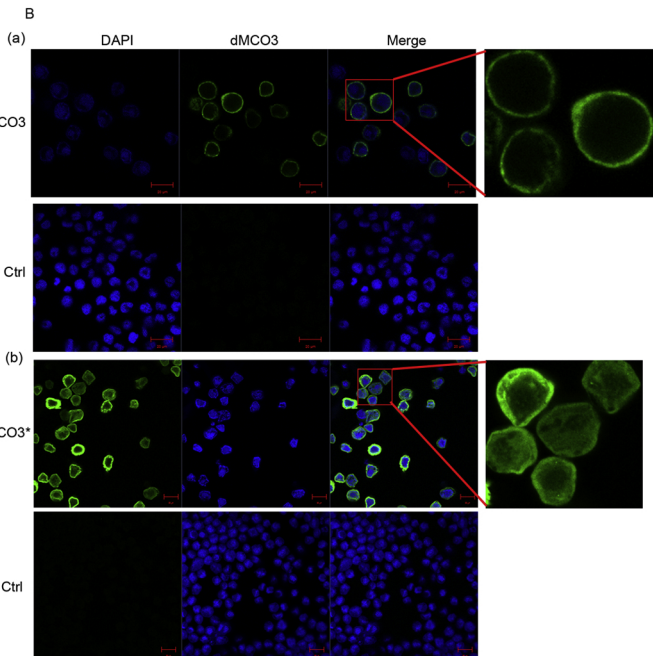
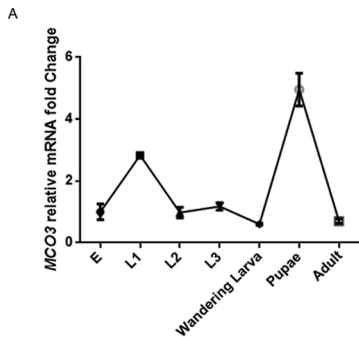


Figure 2



**C**

MGQNFLRRLPANRVASCPWRWFAMSKRESK**SFASLVV**  
**LVLPSPSPS**QCESSKDDFPQAKFEWPSFAWWMIRNK  
 TTGKTFALDLKNDYSQMELANFGDFDRHPCRRVCO  
 QGSGNQNYCYQLVWHNYQRLGSPCCORCQCFDERACA  
 SEHCYGDGVANPVMVAVNRMVPGPSIELCENDTVVV  
 DVLNLYSEPTTMHWGHVHMHRTPEMDGAFFITQYP  
 LQPGEVQRHEFKVDRSGSLWYHSHVGVQQRGFVGA  
 GAFVVRQTSQENQHSQLYDYDLVEHTLMIQDIFEY  
 NLDQVRNILVNGKGRNHSLSQPDNDNRHRYERLRTV  
 PGYRYRMRVILNGIANCPVEFSIEQHLLMISTDGNDI  
 EPVLADGFFLTSAERFDVLEANQYKKNYWRIRKGYE  
 QCENRNIYQGAVLSYRGSARSELPOGDLDKPSSRA  
 ADELDLIVNDFRFKPNASTAISLSRQSLDKDNNVGTV  
 ALRSVDPVPWTRYTKFLTHYSSFGSRTPANGEVLFQI  
 SDISYNSPGISLLQGRHLQDDRYFCNKSLLAAEGR  
 NCERELCECVNVMRLPAYRPLEMVMVANYLDSHTPFH  
 IHGFTFRLVGGQVLGNLNDLRNQLDRRGRRLPRLSE  
 DSAAVAKDTVQIPGGQYIIVRFISNPNPGFWLYHCHVE  
 AHAVQGMVAVLKIGEDHQMKNIAPVRC

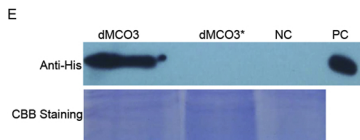
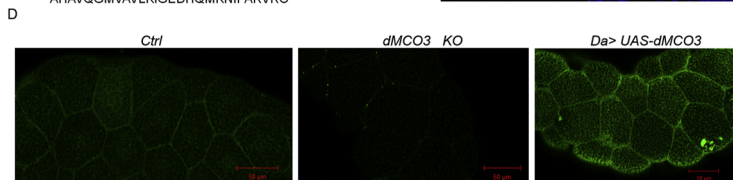


Figure 3

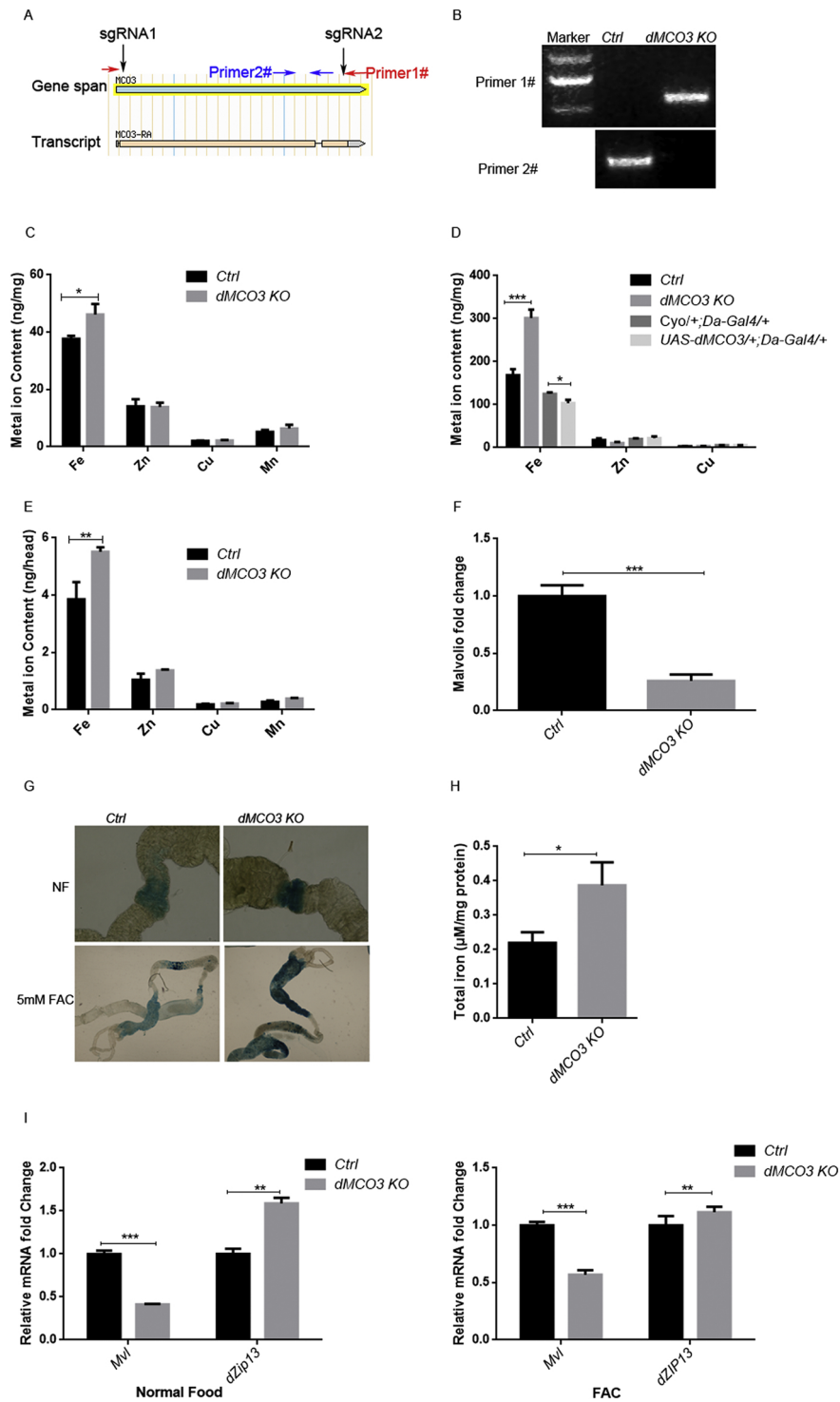


Figure 4

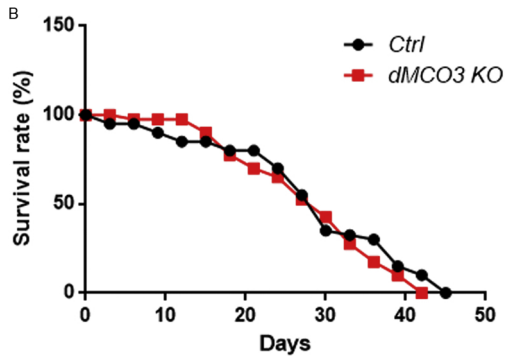
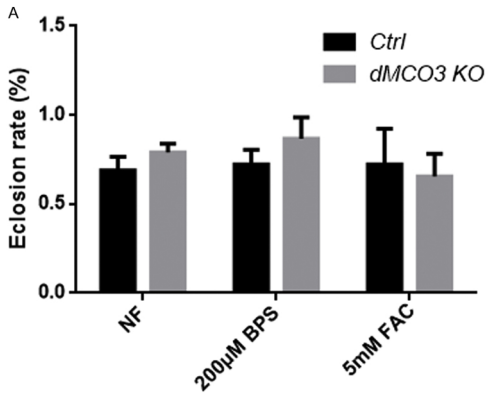


Figure 5